DMD Fast Forward. Published on December 20, 2007 as doi:10.1124/dmd.107.016501

DMD#16501

CYP3A4-MEDIATED CARBAMAZEPINE (CBZ) METABOLISM: FORMATION OF A COVALENT CBZ-CYP3A4 ADDUCT AND ALTERATION OF THE ENZYME KINETIC PROFILE

Ping Kang[‡], Mingxiang Liao, Michael R. Wester, J. Steven Leeder, Robin E. Pearce, and Maria Almira Correia

Departments of Cellular & Molecular Pharmacology, Biopharmaceutical Sciences, Pharmaceutical Chemistry and The Liver Center, University of California, San Francisco, CA (P.K, M.L, and M.A.C),

Pfizer Global Research & Development, San Diego, CA (MRW), and

Section of Developmental Pharmacology and Experimental Therapeutics, The Children's Mercy Hospitals & Clinics, Kansas City, MO (J.S.L and R.E.P)

DMD Fast Forward. Published on December 20, 2007 as DOI: 10.1124/dmd.107.016501
This article has not been copyedited and formatted. The final version may differ from this version.

a) Running Title

Carbamazepine metabolism by CYP3A4

b) Corresponding author

Maria Almira Correia, PhD

Departments of Cellular & Molecular Pharmacology, Biopharmaceutical Sciences, and The Liver Center, University of California, San Francisco

600 16th Street N572F, San Francisco, CA 94158-2280

Telephone: 415-476-3992

Fax: 415-476-5292

Email: almira.correia@ucsf.edu

c) Number of text pages: 34

Number of tables: 1

Number of figures: 5

Number of references: 38

Number of words in the Abstract: 218

Number of words in the Introduction: 459

Number of words in the Discussion: 1493

d) List of nonstandard abbreviations

b_5, cytochrome b_5; CBZ, carbamazepine; MDZ, midazolam; P450 reductase, NADPH-cytochrome P450 reductase; Ni^{2+}-NTA, nickel-nitrilotriacetic acid.

Abstract

Carbamazepine (CBZ) is a widely prescribed anticonvulsant whose use is often associated with idiosyncratic hypersensitivity. Sera of CBZ-hypersensitive patients often contain anti-CYP3A antibodies including those to a CYP3A23 K-helix peptide that is also modified during peroxidative CYP3A4 heme-fragmentation. We explored the possibility that cytochromes P450 (P450s) such as CYP3A4 bioactivate CBZ to reactive metabolite(s) that irreversibly modify the P450 protein. Such CBZ-P450 adducts, if stable *in vivo*, could engender corresponding serum P450 autoantibodies. Incubation with CBZ not only failed to inactivate functionally reconstituted, purified recombinant CYP3A4 or CYP3A4 Supersomes™ in a time-dependent manner, but the inclusion of CBZ (0-1 mM) also afforded a concentration-dependent protection to CYP3A4 from inactivation by NADPH-induced oxidative uncoupling. Incubation of CYP3A4 Supersomes™ with ^{3}H-CBZ resulted in its irreversible binding to CYP3A4 protein with a stoichiometry of 1.58 ± 0.15 pmol ^{3}H-CBZ bound/pmol CYP3A4. Inclusion of GSH (1.5 mM) in the incubation reduced this level to 1.09. Similar binding (1.0 ± 0.4 pmol ^{3}H-CBZ bound/pmol CYP3A4) was observed after ^{3}H-CBZ incubation with functionally reconstituted, purified recombinant CYP3A4$(His)_6$. The CBZ-modified CYP3A4 retained its functional activity albeit at a reduced level, but its testosterone 6β-hydroxylase kinetics were altered from sigmoidal (a characteristic profile of substrate cooperativity) to near-hyperbolic (Michaelis-Menten) type, suggesting that CBZ may have modified CYP3A4 within its active site.

Introduction

Carbamazepine (CBZ), one of the most widely used anticonvulsants, has been associated with a series of idiosyncratic adverse reactions, such as skin rash, blood disorders, hepatotoxicity, and hematological disorders (Leeder, 1998; Shear et al., 1988; Hart and Easton, 1982; Kalapos, 2002; Romero Maldonado et al., 2002). These clinical symptoms are consistent with an immune etiology. Although the mechanism of CBZ-induced adverse reactions has not been well characterized, it is widely believed that biotransformation of CBZ into reactive metabolites and their subsequent covalent binding to cellular proteins is responsible for the immune response (Park et al., 1987).

Bioactivation of CBZ has been found to result in covalent adducts of its metabolites with microsomal proteins (Pirmohamed et al., 1992; Lillibridge et al., 1996). *In vitro* studies with recombinant human P450s expressed in yeast have demonstrated that P450s 1A, 2C, and 3A are responsible for the covalent binding of CBZ to human liver microsomal proteins with 65% and 31% covalent adduct formation attributed to CYP3A4 and CYP1A2, respectively, after normalization of their relative hepatic abundance (Wolkenstein et al., 1998). However, preincubation of human and rat liver microsomes with CBZ in the presence of NADPH with subsequent assay of residual P450 monooxygenation activities provided no evidence for mechanism-based inactivation of rat CYP2C11, CYP3A, CYP1A1/2 or CYP2B1/2 or that of human CYP2C8, CYP2C9 or CYP3A4, whereas time-dependent inactivation of rat CYP2D6 and human CYP1A2 were observed (Masubuchi et al., 2001).

Sera of CBZ-hypersensitive patients often contain anti-CYP3A antibodies including those specific to the CYP3A23 K-helix peptide (EYLDMLNETLRL) (Leeder et al., 1996), a region also modified during peroxidative CYP3A4 heme-fragmentation (He et al., 1998). We explored the possibility that P450s such as CYP3A4 bioactivate CBZ to reactive metabolite(s) that irreversibly modify the P450 protein. Such CBZ-P450 adducts, if stable *in vivo*, could engender corresponding serum P450 autoantibodies if processed and presented to the immune system in an appropriate immunologic context.

Unusual substrate kinetic interactions involving CYP3A4 have been reported, which are proposed to result from the simultaneous binding of multiple substrate molecules and consequent substrate cooperativity within the CYP3A4 active site (Shou et al., 1994; Ueng et al., 1997; Harlow and Halpert, 1998). Covalent modification of CYP3A4 active site has been shown to alter the kinetics of CYP3A4 catalysis, indicating the existence of multiple binding sites (Schrag and Wienkers 2001; Khan et al., 2002). The recently reported crystal structure of CYP3A4 complexed with two molecules of ketoconazole suggested that the atypical kinetics displayed by CYP3A4 could be the result of multiple coexistent binding modes at the active site (Williams et al., 2004; Yano et al., 2004; Ekroos and Sjogren, 2006). The finding that CBZ-modified CYP3A4 still retains considerable functional activity led us to investigate the altered enzyme kinetic profile of CBZ-modified CYP3A4.

DMD Fast Forward. Published on December 20, 2007 as DOI: 10.1124/dmd.107.016501
This article has not been copyedited and formatted. The final version may differ from this version.

Materials and Methods

Materials. CBZ, testosterone, 6β-hydroxytestosterone, GSH, NADPH, EDTA, Hepes, sodium cholate, catalase, magnesium chloride ($MgCl_2$) and ethyl acetate (EtOAc) were purchased from Sigma-Aldrich Co. (St. Louis, MO). [^{3}H]-CBZ was purchased from Amersham Biosciences (Piscataway, NJ). Erythromycin was purchased from Calbiochem (San Diego, CA), and the N-desmethylerythromycin standard was synthesized by Pfizer Inc. (San Diego, CA). L-α-Dilauroylphosphatidylcholine, L-α-dioleyl-*sn*-glycerophosphatidylcholine, and phosphatidyl-serine were purchased from Doosan Serdary Research Laboratories (Englewood Cliffs, NJ). Microsomes (Supersomes™) from baculovirus-infected insect cells expressing CYP3A4 along with co-expressed human NADPH-cytochrome P450 reductase (P450 reductase) and human cytochrome b_5 (b_5) were purchased from BD GENTEST Corp. (Woburn, MA). Ni^{2+}-NTA resin was purchased from Qiagen Inc. (Valencia, CA). The recombinant CYP3A4$(His)_6$ was expressed in *E. coli* DH5αF' cells and purified exactly as described previously (Wang et al., 1998; Xue et al, 2001). Rat liver b_5 and P450 reductase were purified from phenobarbital-pretreated male rat liver microsomes as previously reported (Licad-Coles et al., 1997).

Determination of CBZ covalent binding to functionally reconstituted recombinant CYP3A4: Purified recombinant CYP3A4$(His)_6$, assayed spectrophotometrically (Wang et al., 1998), was functionally reconstituted with P450 reductase and cytochrome b_5 at a previously determined optimal molar ratio of CYP3A4: P450 reductase: b5 of 1:4:2 using testosterone 6β-hydroxylase as the functional probe as described (Wang et al., 1998). The reagents were added at 4°C in the following order in a final volume of 1 mL: Lipid mixture (L-α-dilauroylphosphatidylcholine: L-

DMD Fast Forward. Published on December 20, 2007 as DOI: 10.1124/dmd.107.016501
This article has not been copyedited and formatted. The final version may differ from this version.

α-dioleyl-sn-glycerophosphatidylcholine: phosphatidyl-serine, 1:1:1, w/w, 20 μg), sodium cholate (200 μg), cytochrome b_5 (500 pmol), P450 reductase (1000 pmol), CYP3A4 (250 pmol), and GSH (1.5 μmol). The mixture was reconstituted at room temperature for 10 min, and then placed back on ice. The following reagents were then added in order to a final volume of 1 mL: Hepes (50 mM, pH 7.85), 20% glycerol, catalase (200 u), EDTA (1 mM), water, $MgCl_2$ (30 mM), and CBZ with [^{3}H]CBZ (1 mM and 1.25 μCi/mL final, dissolved in methanol). Following a 3 min-preincubation at 37°C, NADPH (1 mM final) was added to initiate the reaction. Controls for non-specific binding were prepared as described except that the incubations contained no NADPH. Carrier rat liver microsomal protein (10 mg) was added after a 30 min-incubation, and the incubation was immediately quenched with EtOAc. The protein precipitate was then washed thrice with methanol containing 5% H_2SO_4, followed by three washes with a mixture of ethanol and ethyl ether (3:1, v/v)**,** and two washes with 80% aqueous methanol. The pellet was dissolved in 1 N NaOH. An aliquot was neutralized with 1 N HCl, and liquid scintillation fluid was added for radioactivity determination. The protein concentration of another aliquot was also determined to calculate the protein recovery. The stoichiometry of covalent binding was determined on the basis of the recovered residual radioactivity irreversibly bound to the precipitated protein pellet. Higher concentrations of GSH up to 4 mM were also included in the incubation mixture to study the effect of GSH on the covalent binding.

Determination of CBZ-covalent binding to CYP3A4 Supersomes™:

A mixture of CYP3A4 Supersomes™ (100 pmol), isocitric acid (5 mM), isocitric acid dehydrogenase (0.5 U/mL), potassium phosphate buffer (100 mM, pH 7.4), CBZ with [^{3}H]CBZ (1 mM and 1.25 μCi/mL final, dissolved in methanol), and EDTA (1 mM) was preincubated for

DMD Fast Forward. Published on December 20, 2007 as DOI: 10.1124/dmd.107.016501
This article has not been copyedited and formatted. The final version may differ from this version.

3 min at 37°C. NADPH (1 mM, final) was added to start the reaction (final volume, 0.5 ml). Controls for non-specific binding consisted of exactly similar incubations without NADPH. Carrier microsomal protein (10 mg) was added after a 30 min-incubation and the reaction was terminated with EtOAc. The protein pellet was washed as detailed above. The stoichiometry of covalent binding was calculated on the basis of the recovered residual radioactivity irreversibly bound to the protein pellet as described above. When the effect of GSH on the CBZ covalent binding to CYP3A4 was assessed, GSH up to 4 mM was also included in the incubation mixture.

Reisolation of [^{3}H]CBZ-CYP3A4(His)$_6$ adduct:

Following a 30 min-incubation of the functionally reconstituted recombinant CYP3A4(His)$_6$ with [^{3}H]CBZ as described above, the incubation mixture was mixed with pre-equilibrated Ni^{2+}-NTA resin and then loaded onto a column. After removal of free [^{3}H]CBZ by extensive washing with Hepes buffer (50 mM, pH 7.85) containing 20 mM imidazole, the [^{3}H]CBZ-CYP3A4(His)$_6$ adduct was eluted out of the column with the same buffer containing 200 mM imidazole. The purified [^{3}H]CBZ-CYP3A4(His)$_6$ adduct was subjected to SDS-PAGE analyses, and the protein quantified by densitometry relative to the content of the purified CYP3A4 used as the starting material and electrophoresed in parallel. The stoichiometry of covalent binding was calculated on the basis of the residual radioactivity irreversibly bound to the recombinant CYP3A4 protein.

Testosterone 6β-hydroxylase activity of the CBZ-modified CYP3A4:

After a 30 min-incubation of CBZ with either CYP3A4 Supersomes™ or the functionally reconstituted purified recombinant CYP3A4 as described above, an aliquot of CYP3A4 (10 pmol) was added to a secondary reaction mixture (1 mL final volume) containing testosterone

(1.9 μM to 500 μM) and other reagents as described above. The reaction was initiated by the addition of NADPH (1 mM), allowed to run at 37°C for 20 min, and then quenched with EtOAc. Progesterone was included as an internal control. The metabolites were extracted twice with EtOAc, dried down under N_2, and assayed by HPLC with peak area quantification for 6β-hydroxytestosterone, the major product, as described previously (Xue et al., 2001).

Kinetic analysis of CYP3A4 6β-hydroxylation of testosterone was performed using the Hill Equation:

$$\upsilon = V_{max}/[1 + (K_m/C)^n]$$

where υ is the enzyme velocity, C is the substrate concentration, K_m is the substrate concentration at the half maximum velocity, n is the Hill coefficient, and V_{max} is the maximal velocity. The non-linear, least-squares curve fitting was carried out with Igor Pro 4.01 (WaveMetrics, Inc, OR).

Time-dependent inhibition of CYP3A4 testosterone hydroxylase activity:

Functionally reconstituted, purified recombinant CYP3A4 was incubated with various concentrations of CBZ (0-1000 μM) at 37°C as described above. Aliquots of the mixtures (40 μL containing 10 pmol CYP3A4) were taken at various time intervals (0-20 min) and added to a secondary reaction mixture (1 mL final volume) containing 250 μM testosterone, Hepes (50 mM, pH 7.85), 20% glycerol, catalase (200 u), EDTA (1 mM), GSH (1.5 mM), and $MgCl_2$ (30 mM) for the determination of the residual testosterone 6β-hydroxylase activity as described above. CYP3A4 Supersomes™ were incubated with 150 μM and 1000 μM of CBZ at 37°C as described above. Aliquots of the mixtures (100 μL containing 10 pmol CYP3A4) were taken at various time intervals (0-30 min) and added to a secondary 1 mL reaction mixture containing 250 μM

testosterone, isocitric acid (5 mM), isocitric acid dehydrogenase (0.5 U/mL), potassium phosphate buffer (100 mM, pH 7.4), EDTA (1 mM), and GSH (1.5 mM) for the determination of the residual testosterone 6β-hydroxylase activity as described above.

Erythromycin N-demethylase activity of the CBZ-modified CYP3A4: After a 30 min-incubation of CBZ with CYP3A4 Supersomes™ as described above, an aliquot of CYP3A4 (1 pmol) was added to a secondary reaction mixture (0.2 mL, final volume) containing erythromycin (1 to 350 μM) and other reagents as described above. The reaction was initiated by the addition of NADPH (1 mM), allowed to run at 37°C for 15 min, and then quenched with 0.2 mL acetonitrile. A 10 μL-aliquot was subjected to liquid chromatography-mass spectrometric (LC-MS) analyses for metabolite quantification. N-desmethylerythromycin was quantified by Shimadzu LC-10AD VP binary pumps (Shimadzu, Columbia, MD) coupled with a Q-Trap 4000 (Applies Biosystems/MSD Sciex, Concord, ON, Canada). The metabolite was separated by a Synergi Fusion-RP column (4 μm, 100 x 2.0 mm, Phenomenex, Torrance, CA) at a flow rate of 0.2 mL/min. A gradient of (A) water with 0.1% formic acid and (B) acetonitrile with 0.1% formic acid was applied as follows: initiated with 20% B for 1 min and then increased in a linear manner to 65% at 2.3 min and to 100% at 4.5 min. The gradient was maintained at 100% B for 5 min and then decreased to 20% at 5.5 min. The column was allowed to equilibrate at 20% solvent B for 0.5 min prior to the next injection. The HPLC effluent going to the mass spectrometer was directed to waste through a divert valve for the initial 1 min after sample injection. The Q-trap 4000 electrospray-MS was operated in the positive ionization mode, by applying to the capillary a voltage (IS) of 4.5 kV. Nitrogen was used as curtain gas (CUR), as well as nebulizing (GS1) and turbo spray gas (GS2, heated at 450 C), with the optimum values

set, respectively, at 36, 50, and 40 (arbitrary values). Collision-activated dissociation (CAD) was performed at 6 (arbitrary value) with nitrogen as collision gas. Declustering potential (DP) was set at 41 V, whereas entrance potential (EP) was set at 10 V; collision energy (CE) was optimized at 51 eV. The multiple reaction monitoring (MRM) transitions used were 720→144 for N-desmethylerythromycin. The concentrations were determined by means of a standard curve, wherein N-desmethylerythromycin was dissolved in the same incubation and quench buffer to prepare standards with concentrations ranging from 0.1 to 100 μg/mL. Kinetic data analyses of CYP3A4-dependent erythromycin N-demethylase were performed as described above for testosterone 6β-hydroxylase.

Flexible docking of CBZ, testosterone and erythromycin in CYP3A4 crystal structure:

Initial flexible docking of testosterone into the active site of CYP3A4 [Protein Data Bank accession codes 1w0g (Williams et al., 2004)] was carried out with FlexX, version 1.7.6, implemented in the SYBYL, version 7.0 (Tripos, Inc. St. Louis, MO.). The docking solutions were ranked according to CScore. Visual inspection identified a low energy binding mode compatible with 6β-hydroxylation of testosterone and this protein-ligand complex was used as a starting point for further flexible docking experiments with testosterone or CBZ using the Pfizer in-house docking and scoring software (Gehlhaar et al., 1995; Gehlhaar et al, 1999; Marrone et al, 1999). Restrained docking of CBZ into the active site of the previously identified complex anchoring its 2, 3, 10 or 11 carbon near the sulfur of Cys239 was performed and followed by protein-ligand minimization to yield a low energy binding mode. In separate experiments, a second testosterone was docked into the previously identified 3A4-testosterone complex using a method that allowed the protein to move throughout the docking simulation via discrete

minimization. Erythromycin was also docked into the 1w0g structure using a restrained docking method that anchored the site of metabolism near the heme iron and was followed by a docking simulation that allowed protein flexibility.

Results

Time-dependent inactivation of CYP3A4 testosterone 6β-hydroxylase activity by CBZ:

The testosterone 6β-hydroxylase activity of both CYP3A4 Supersomes™ and functionally reconstituted purified recombinant CYP3A4(His)$_6$ was reduced with increasing preincubation time with CBZ (Fig**.** 1A and Fig. 1B). However, the time-dependent functional inactivation of CYP3A4 was not exacerbated by increasing concentrations of CBZ. Instead, the greatest inactivation of enzyme activity particularly with the functionally reconstituted purified recombinant CYP3A4, was observed in the absence of CBZ (Fig. 1B), and inclusion of CBZ increasingly protected the enzyme from time-dependent inactivation. Functionally reconstituted recombinant CYP3A4(His)$_6$ incubated with NADPH alone also showed a significant reduction in its characteristic reduced CO-binding 450 nm-absorption spectrum (data not shown). These findings do not support the mechanism-based inactivation of CYP3A4 by CBZ; however, they are consistent with significant oxidative uncoupling associated with these CYP3A4 systems containing a 1:4 molar excess of P450 reductase, in the absence of substrates.

Determination of CBZ-covalent binding to CYP3A4 protein:

Incubation of CYP3A4 Supersomes™ with [^{3}H]CBZ resulted in covalently bound CBZ to CYP3A4. After extensive organic solvent washes to remove free nonspecifically bound [^{3}H]CBZ, the residual radioactivity associated with the protein pellet was monitored. The stoichiometry (molar ratio) of CBZ:CYP3A4 protein was calculated to be 1.58 : 1. Inclusion of GSH (1.5 mM) in the incubation reduced this molar ratio to 1.09. Similar covalent binding analyses with the recombinant CYP3A4, functionally reconstituted in the presence of GSH (1.5 mM), and using

DMD Fast Forward. Published on December 20, 2007 as DOI: 10.1124/dmd.107.016501
This article has not been copyedited and formatted. The final version may differ from this version.

the same protein precipitation method, yielded a stoichiometry of CBZ-CYP3A4 adduct of 0.79:1.

Determination of the covalent binding by re-isolation of the CBZ-CYP3A4(His)$_6$ adduct:

The stoichiometry of the adduct was also determined by isolating the CBZ-modified CYP3A4(His)$_6$ protein after incubation of the functionally reconstituted recombinant CYP3A4(His)$_6$ with [^{3}H]CBZ, by Ni^{2+}-NTA affinity chromatography. Unbound CBZ and other constituents of the incubation mixture such as P450 reductase and b_5 were removed by extensive washing, as monitored by SDS-PAGE analyses, which showed that the residual radioactivity was associated solely with the eluted CYP3A4(His)$_6$, and that the CBZ-CYP3A4(His)$_6$ adduct was clearly separated from P450 reductase and b_5. The stoichiometry of the isolated CBZ-CYP3A4(His)$_6$ adduct was calculated to be 1 ± 0.4 pmol CBZ/pmol CYP3A4 on the basis of its residual radioactivity. Together, these findings indicated that the bioactivated CBZ covalently modified CYP3A4, possibly within the active site of this enzyme to form a CBZ-CYP3A4 protein adduct.

Enzyme kinetics of CBZ-modified CYP3A4:

Influence on testosterone 6β-hydroxylation: To explore the possible site of CBZ adduction, its effect on the cooperativity with a known CYP3A4 substrate testosterone was probed. Incubation of CYP3A4 Supersomes™ with testosterone, yielded the previously reported sigmoidal kinetics as evidenced by the curved Eadie-Hofstee plot (Fig. 2A, n = 1.2). The kinetic values obtained after the data were fitted to the Hill equation are shown in Table 1A. CYP3A4-dependent testosterone 6β-hydroxylase activity was inhibited when CYP3A4 was preincubated with CBZ in

the presence or absence of NADPH. When preincubated with CBZ in the absence of NADPH, CYP3A4 still retained its sigmoidal kinetics (Fig. 2B, n = 1.3). In contrast, after preincubation with NADPH, which, as described above, results in a covalent 1:1 molar CBZ-adduction of CYP3A4, the CBZ-modified enzyme displayed an almost hyperbolic kinetic profile of testosterone 6β-hydroxylation (Fig. 2C, n = 1.0). The K_m for testosterone was unaffected when CYP3A4 was preincubated with CBZ without NADPH. A larger increase in K_m was observed when CYP3A4 was covalently modified by CBZ in the presence of NADPH. However, the V_{max} values albeit lower, were not substantially different after preincubation with CBZ in the presence or absence of NADPH (Table 1A).

A similar sigmoidal kinetic profile, characterized by a curved Eadie-Hofstee plot (Fig. 3A, n = 1.4) was also observed for the testosterone 6β-hydroxylase activity of functionally reconstituted recombinant CYP3A4. The rate of 6β-hydroxytestosterone formation was inhibited in the presence of CBZ, even in the absence of NADPH. Eadie-Hofstee analyses of the enzyme activity in the presence of CBZ but without preincubation with NADPH revealed a similar sigmoidal profile, although the presence of CBZ lowered the Hill coefficient (Fig. 3B, n = 1.2). The K_m of testosterone increased in the presence of CBZ, thereby suggesting CBZ competition at the testosterone-binding site. After covalent modification of CYP3A4 by preincubation with CBZ in the presence of NADPH, its residual testosterone 6β-hydroxylase activity yielded an almost hyperbolic profile with a linear Eadie-Hofstee plot (Fig. 3C). The Hill coefficient n also decreased to 1.1 (Table 1A). CBZ-modified CYP3A4 also displayed a lower binding affinity towards testosterone as evidenced by the increased K_m value, whereas the V_{max} value only slightly decreased when NADPH was included in the preincubation (Table 1A).

Influence on erythromycin N-demethylation: To further assess the effect of covalent CBZ-induced modification on CYP3A4-dependent function, the N-demethylation of erythromycin, another prototypic CYP3A4 substrate with an affinity comparable to that of testosterone and thus a competitive substrate inhibitor of CYP3A4-dependent testosterone 6β-hydroxylase activity (Wang et al., 1997), was examined. However, the kinetic data obtained for erythromycin N-demethylation after CBZ-induced modification of CYP3A4 Supersomes™ were scattered and failed to provide a good fit to either the Hill equation or Michaelis-Menten equation. Nevertheless, curve fitting yielded comparable Vmax values for CYP3A4-dependent erythromycin N-demethylation with (3.61 ± 0.22 nmol/nmol CYP3A4/min) or without (3.60 ± 0.58 nmol/nmol CYP3A4/min) CBZ-induced covalent modification of the enzyme (Fig. 4A-C; Table 1B). These results suggested that contrary to the results obtained with testosterone as a substrate, CBZ-induced covalent modification of CYP3A4 had no significant effect on erythromycin N-demethylation.

Flexible docking of CBZ, testosterone and erythromycin in CYP3A4 crystal structure:

Initial dockings with testosterone into the active site of apo CYP3A4 identified a low energy binding pose of testosterone near the heme that is consistent with its 6β-hydroxylation. This complex was used as the starting point for further docking experiments. When a second molecule of testosterone is docked into the active site using an induced fit method which allows minimal protein flexibility during docking, one of the low energy binding modes places the second testosterone partly in the active site but extending toward the surface of the protein in a channel that is defined by the helix G' to helix G loop, the B-C loop and the I helix. This docking did not require any repositioning of the 1st testosterone bound (Fig. 5A).

Restrained docking of CBZ yielded poses which would be compatible with adduct formation with Cys239 by carbon 2 or 3 of CBZ (Fig. 5A). Furthermore, low energy binding modes were also observed when the 10 or 11 carbon of CBZ was restrained toward Cys239 suggesting that adduct formation arising from the 10,11-epoxide intermediate is also possible (data not shown). All of the restrained docking binding poses observed for CBZ, regardless of which carbon was anchored, are compatible with testosterone binding near the heme, but would cause steric clashes with a 2nd molecule of testosterone bound in the active site as described previously (Fig. 5A). On the other hand, restrained docking of erythromycin in the apo active site of 1w0g yielded a low energy-binding pose that allowed approach of its dimethylamino nitrogen consistent with the known N-demethylation of erythromycin by CYP3A4 (Fig. 5B).

Discussion

In vitro studies with recombinant human P450s expressed in yeast have documented the covalent binding of CBZ to proteins belonging to the P450 subfamilies 1A, 2C, and 3A (Wolkenstein et al., 1998). However, no mechanism-based inactivation of the covalently modified P450s was detected. Similarly, no evidence for the functional inactivation of human CYP2C8, CYP2C9 or CYP3A4 could be found after preincubation of human liver microsomes with CBZ in the presence of NADPH (Masubuchi et al., 2001). In the present study, we show that CYP3A4 Supersomes™ formed an adduct with [^{3}H]CBZ with a molar stoichiometry of 1.58: 1 (CBZ: CYP3A4). This molar ratio was reduced to about 1:1 by inclusion of GSH (1.5 mM) in the incubation; however, this molar ratio was not further affected by higher concentrations of GSH (up to 4 mM). Since both CYP3A4 Supersomes™ and yeast microsomes contain various other proteins, the possibility existed that proteins other than CYP3A4 were covalently modified by CBZ and thus either were acid co-precipitated with CYP3A4, or co-migrated with it after SDS-PAGE. We therefore examined a simpler system consisting of purified functionally reconstituted CYP3A4, wherein after incubation with CBZ, the CBZ-modified recombinant CYP3A4(His)$_6$ was readily separated from P450 reductase and b_5 by Ni^{2+}-NTA affinity chromatography. A similar 1:1 molar ratio was observed in this CBZ-modified CYP3A4(His)$_6$ system, thus suggesting that CYP3A4 expressed in baculovirus (CYP3A4 Supersomes™) and yeast (Wolkenstein et al., 1998) was most likely the only protein that was covalently modified by CBZ. The fact that GSH (1.5 mM) normally included in CYP3A4 functional reconstitution systems, failed to reduce this 1:1 molar ratio of CBZ:CYP3A4 suggested that CBZ was covalently bound within the CYP3A4 active site, thereby making it somewhat inaccessible for nucleophilic trapping by GSH.

DMD Fast Forward. Published on December 20, 2007 as DOI: 10.1124/dmd.107.016501
This article has not been copyedited and formatted. The final version may differ from this version.

We find it noteworthy however, that a considerably greater extent of CBZ-induced covalent binding occurs in the absence of GSH. This suggests that individuals with low hepatic GSH content, which may result from pharmacological depletion by coadministered drugs, dietary deprivation, inadequate repletion of GSH-precursors, or even defective GSH synthesis, may be at a higher risk for enhanced covalent modification of P450s. Subsequent proteolytic processing of such CBZ-modified P450s for antigenic presentation may contribute to the pathogenesis of the hypersensitivity/idiosyncratic reactions. Although the mechanism of CBZ bioactivation and covalent binding has yet to be precisely elucidated, previous studies have suggested that a CBZ-derived arene oxide, quinone, iminoquinone, catechol, quinone methide and/or epoxide could be viable reactive metabolites that chemically modify P450s (Madden et al., 1996; Pearce et al., 2002; Pearce et al., 2005, 2007; Bu et al., 2005) (Scheme 1). Furthermore, although the precise site of this binding remains to be identified, conceivably Cys239 could be a plausible target as in raloxifene-mediated CYP3A4 adduction (Baer et al., 2007). Nevertheless, our finding that CBZ covalently modifies CYP3A4 (possibly at the active site) is intriguing in view of the fact that it maims but does not inactivate the enzyme, consistent with the report that CBZ is not a mechanism-based CYP3A4 inactivator (Masubuchi et al, 2001).

The unusual sigmoidal kinetic interactions exhibited by CYP3A4 have been rationalized by the binding of multiple substrate molecules at more than one site within the CYP3A4 active site (Shou et al., 1994; Harlow and Halpert, 1998; Ueng et al., 1997; Korzekwa et al., 1998). Similar sigmoidal kinetics of CYP3A4-catalyzed CBZ metabolism implies multiple CBZ-binding sites within the CYP3A4 active site **(**Nakamura et al., 2003**).** However, the observed 1:1 molar

stoichiometry of the CBZ-CYP3A4 adduct suggests that only one substrate binding site of CYP3A4 was covalently modified by CBZ, with the other CBZ-binding sites remaining unscathed. Furthermore, not only was the CYP3A4-characteristic testosterone 6β-hydroxylase activity only slightly reduced when CYP3A4 was covalently modified by CBZ, but such modification also failed to affect CYP3A4-dependent erythromycin N-demethylase activity. CBZ also fails to functionally inactivate CYP3A4 in a mechanism-based manner in human liver microsomes (Masubuchi et al., 2001). Indeed, the presence of endogenous steroids such as testosterone in the incubation, drastically increases CYP3A4-dependent CBZ 10,11-epoxidase activity, and alters its kinetic profile from sigmoidal to hyperbolic (Michaelis-Menten type) (Nakamura et al., 2003). Such substrate cooperativity at the CYP3A4 active site was taken as evidence for a two-site substrate-binding model. Consistent with this model, our study showed that a complete block of one CYP3A4 substrate-binding site by CBZ covalent modification altered the kinetic profile of CYP3A4-dependent testosterone 6β-hydroxylation from sigmoidal to near-hyperbolic (Michaelis-Menten type). Due to the higher CYP3A4 binding affinity of testosterone (K_m, 30-100 μM) than that of CBZ (K_m, 250 μM) (Pelkonen et al. 2001), CBZ does not compete effectively for all the CYP3A4-testosterone substrate binding sites, thus leading to the retention of its CYP3A4 sigmoidal kinetic profile. Interestingly, CBZ inclusion led to a greater reduction of the Hill coefficient for the functionally reconstituted purified CYP3A4$(His)_6$ (n = 1.4 to n = 1.2) but an increase for CYP3A4 Supersomes™ (from n = 1.2 to n = 1.3), which may be explained by the higher binding affinity of testosterone to CYP3A4 Supersomes™ (K_m= 41.0 μM) than to the functionally reconstituted purified CYP3A4$(His)_6$ (K_m = 81.5 μM).

In silico docking studies were undertaken in an attempt to rationalize the effect of CBZ-modification of CYP3A4 on its atypical testosterone 6β-hydroxylation kinetics. While the presence of multiple binding sites and consequent substrate cooperativity within the CYP3A4 active site is supported by the simultaneous docking of both α-napthoflavone and testosterone into the apo crystal structure, the recently reported CYP3A4 crystal structure with two complexed ketoconazole molecules confirms that the CYP3A4 active site can simultaneously accommodate even relatively large substrate ligands (Yano et al., 2004) (Ekroos et al., 2006). In a similar manner, our *in silico* experiments suggest that at least two molecules of testosterone can simultaneously bind in the CYP3A4 active site. One testosterone is bound near the heme in an orientation compatible with its 6β-hydroxylation and a second extends toward the surface of the protein via an access channel, that also contains Cys239 located on the loop between helix G' and helix G (Fig. 5). In the absence of any large conformational alterations upon adduct formation, CBZ bound at Cys239 would sterically hinder testosterone binding at this second site but would not affect its catalytic binding near the heme. The persistence of a relatively robust testosterone 6β-hydroxylase activity after CBZ-modification of the CYP3A4 active site is thus consistent not only with the successful simultaneous docking of both CBZ and testosterone therein, but also the plausible existence of multiple binding sites within the capacious CYP3A4 active site. Indeed, this particular CYP3A4 feature is further underscored by our findings that the N-demethylation of erythromycin is largely unaffected by CBZ-induced CYP3A4 covalent modification. Our docking analyses reveal that this relatively large macrolide apparently assumes a slightly different orientation within the CYP3A4 active site, that would be unaffected by the CBZ-modification in the access channel, thereby precluding any steric/kinetic effects such as those observed with testosterone 6β-hydroxylation (Fig. 5B).

Intriguingly however, such CBZ-mediated alteration of testosterone hydroxylation kinetic profile from sigmoidal to near hyperbolic following its CYP3A4 active site modification, may rationalize the reported failure of midazolam (MDZ) hydroxylation to exhibit any detectable homotropic cooperativity (Khan et al., 2002), in spite of its putative binding at multiple sites within the CYP3A4 active site. The covalent modification of one of these sites during its mechanism-based inactivation via 1'-OH MDZ formation may similarly conceal its sigmoidal kinetic profile. Moreover, such MDZ-mediated covalent modification is reported to differentially inhibit CYP3A4-catalyzed oxidations of testosterone and triazolam, thereby providing further evidence for the possible existence of multiple spatially distinct binding sites or binding orientations for each of these substrates (Schrag and Wienkers. 2001; Khan et al., 2002). Additional evidence for plausible MDZ binding at two distinct albeit overlapping CYP3A4 active sites may be derived from the findings of its regioselective hydroxylation to either 1'-OH MDZ or 4-OH MDZ by CYP3A4 and several of its active site-directed mutants (Khan et al., 2002).

Lastly, it is to be noted that significant time-dependent enzyme inactivation of both CYP3A4 Supersomes™ and functionally reconstituted purified recombinant CYP3A4$(His)_6$ was observed upon incubation with NADPH alone, consistent with marked oxidative uncoupling associated with these CYP3A4 systems in the absence of substrates (Denisov et al., 2006; Zangar et al., 2004). Interestingly, CBZ inclusion in these incubations protected CYP3A4 from this time-dependent inactivation, and this protection was magnified by increasing CBZ concentrations,

thereby precluding the detection of any CBZ-induced mechanism-based inactivation of CYP3A4 testosterone 6β-hydroxylase activity.

In summary, CYP3A4-mediated bioactivation of CBZ generated a covalent CBZ-CYP3A4 adduct with a molar ratio of 1:1 (CBZ:CYP3A4). The formation of this drug-protein adduct could not be abolished by GSH inclusion. However, the CBZ-modified CYP3A4 was still functionally active albeit at a reduced functional level with testosterone as the substrate. This CYP3A4 covalent modification by CBZ altered its testosterone 6β-hydroxylase kinetic profile from sigmoidal to near-hyperbolic Michaelis-Menten type, thereby suggesting that CBZ-mediated modification occurs within the CYP3A4 active site.

Acknowledgments:

The authors wish to thank Dr. Xin He, Incyte Corp., for the valuable discussions and assistance with the initial flexible docking analysis and Prof. Paul Ortiz de Montellano, UCSF, for the use of his Silicon Graphics station and FlexX software. We thank Dr. Bernard Murray, Gilead Sciences Inc., for bringing the Baer et al. findings to our attention. We also acknowledge the UCSF Liver Core Center Facilities on Molecular Analyses (Spectrophotometry) supported by P30DK26743.

References

Baer BR, Wienkers LC, Rock DA. (2007) Time-dependent inactivation of P450 3A4 by raloxifene: identification of Cys239 as the site of apoprotein alkylation. *Chem Res Toxicol.* **20**:954-964. Epub 2007 May 12

Bu HZ, Kang P, Deese AJ, Zhao P, Pool WF. (2005) Human in vitro glutathionyl and protein adducts of carbamazepine-10,11-epoxide, a stable and pharmacologically active metabolite of carbamazepine. *Drug Metab Dispos.* **33**:1920-4.

Denisov, I. G., Grinkova, Y. V., Baas, B. J., and Sligar, S. G. (2006) The ferrous-dioxygen intermediate in human cytochrome P450 3A4. Substrate dependence of formation and decay kinetics, *J Biol Chem* **281**, 23313-23318.

Ekroos M, Sjogren T. (2006) Structural basis for ligand promiscuity in cytochrome P450 3A4. *Proc Natl. Acad. Sci. USA.* **103**:13682-13687.

Gehlhaar, D., Bouzida, D., and P. A. Rejto (1999) Reduced Dimensionality in Ligand-Protein Structure Prediction: Covalent Inhibitors of Serine Proteases and Design of Site-Directed Combinatorial Libraries. *ACS Symposium Series 719: Rational Drug Design.* Parrill, A. L. and M. R. Reddy, eds. ACS Press. 292-311.

Gehlhaar, D. K., Verkhivker, G. M., Rejto, P. A., Sherman, C. J., Fogel, D. B., Fogel, L. J., and S. T. Freer. (1995) Molecular recognition of the inhibitor AG-1343 by HIV-1 protease: conformationally flexible docking by evolutionary programming. *Chem. & Bio.* **2:** 317-324.

Harlow G. R., Halpert J. R. (1998) Analysis of human cytochrome P450 3A4 cooperativity: construction and characterization of a site-directed mutant that displays hyperbolic steroid hydroxylation kinetics. *Proc Natl. Acad. Sci*. USA; 95:6636-41.

Hart RG, Easton JD. (1982) Carbamazepine and hematological monitoring. *Ann Neurol*. **11**:309-12.

He K, Bornheim LM, Falick AM, Maltby D, Yin H, Correia MA. (1998) Identification of the heme-modified peptides from cumene hydroperoxide-inactivated cytochrome P450 3A4. *Biochemistry*. **37**:17448-57.

Kalapos M. P. (2002) Carbamazepine-provoked hepatotoxicity and possible aetiopathological role of glutathione in the events. Retrospective review of old data and call for new investigation. *Adverse Drug React Toxicol Rev*. **21**:123-41.

Khan K. K., He Y. Q., Domanski T. L., Halpert J. R. (2002) Midazolam oxidation by cytochrome P450 3A4 and active-site mutants: an evaluation of multiple binding sites and of the metabolic pathway that leads to enzyme inactivation. *Mol. Pharmacol.*; **61**: 495-506.

Korzekwa KR, Krishnamachary N, Shou M, Ogai A, Parise RA, Rettie AE, Gonzalez FJ, Tracy TS. (1998) Evaluation of atypical cytochrome P450 kinetics with two-substrate models: evidence that multiple substrates can simultaneously bind to cytochrome P450 active sites. *Biochemistry*. **37**:4137-47.

Leeder J. S. (1998) Mechanisms of idiosyncratic hypersensitivity reactions to antiepileptic drugs. Epilepsia. **39** Suppl 7:S8-16.

Leeder JS, Gaedigk A, Lu X, Cook VA. (1996) Epitope mapping studies with human anti-cytochrome P450 3A antibodies. *Mol Pharmacol*. **49**:234-43.

Licad-Coles E, He K, Yin H, Correia MA. (1997) Cytochrome P450 2C11: Escherichia coli expression, purification, functional characterization, and mechanism-based inactivation of the enzyme. *Arch Biochem Biophys.* **338**:35-42.

Lillibridge JH, Amore BM, Slattery JT, Kalhorn TF, Nelson SD, Finnell RH, Bennett GD. (1996) Protein-reactive metabolites of carbamazepine in mouse liver microsomes. *Drug Metab Dispos*. **24**:509-14.

Madden S, Maggs JL, Park BK. (1996) Bioactivation of carbamazepine in the rat in vivo. Evidence for the formation of reactive arene oxide(s). *Drug Metab Dispos*. **24**:469-79.

Marrone, TJ, Luty, BA, Rose, PW. (1999) Discovering high-affinity ligands from the computationally predicted structures and affinities of small molecules bound to a target: A virtual screening approach. *Virtual Screening: An Alternative or Complement to High Throughput Screening? Proceedings of the Workshop 'New Approaches in Drug Design and Discovery', special topic 'Virtual Screening', Schloß Rauischholzhausen, Germany, March 15–18, 1999,* Springer Netherlands. 209-230.

Masubuchi Y, Nakano T, Ose A, Horie T. (2001) Differential selectivity in carbamazepine-induced inactivation of cytochrome P450 enzymes in rat and human liver. *Arch Toxicol*. **75**:538-43.

Nakamura H, Torimoto N, Ishii I, Ariyoshi N, Nakasa H, Ohmori S, Kitada M. (2003) CYP3A4 and CYP3A7-mediated carbamazepine 10,11-epoxidation are activated by differential endogenous steroids. *Drug Metab Dispos*. **31**:432-8.

Park BK, Coleman JW, Kitteringham NR. (1987) Drug disposition and drug hypersensitivity. *Biochem Pharmacol*. **36**:581-90.

Pearce RE, Uetrecht JP, Leeder JS. (2005) Pathways of carbamazepine bioactivation in vitro: II. The role of human cytochrome P450 enzymes in the formation of 2-hydroxyiminostilbene. *Drug Metab Dispos*. **33**:1819-26.

Pearce RE, Vakkalagadda GR, Leeder JS. (2002) Pathways of carbamazepine bioactivation in vitro I. Characterization of human cytochromes P450 responsible for the formation of 2- and 3-hydroxylated metabolites. *Drug Metab Dispos*. **30**:1170-9.

Pearce RE, Lu W, Wang Y-Q, Uetrecht JP, Correia MA, Leeder JS. (2007) Pathways of carbamazepine bioactivation in vitro III. The role of human cytochrome P450 enzymes in the formation of 2,3-dihydroxycarbamazepine. *(Submitted)*

Pelkonen O, Myllynen P, Taavitsainen P, Boobis AR, Watts P, Lake BG, Price RJ, Renwick AB, Gomez-Lechon MJ, Castell JV, Ingelman-Sundberg M, Hidestrand M, Guillouzo A, Corcos L, Goldfarb PS, Lewis DF. (2001) Carbamazepine: a 'blind' assessment of CVP-associated metabolism and interactions in human liver-derived in vitro systems. *Xenobiotica*. **31**(6):321-43.

Pirmohamed M, Kitteringham NR, Breckenridge AM, Park BK. (1992) The effect of enzyme induction on the cytochrome P450-mediated bioactivation of carbamazepine by mouse liver microsomes. *Biochem Pharmacol*. **44**:2307-14.

Romero Maldonado N, Sendra Tello J, Raboso Garcia-Baquero E, Harto Castano A. (2002) Anticonvulsant hypersensitivity syndrome with fatal outcome. *Eur J Dermatol*. **12**:503-5.

Schrag M. L., Wienkers L. C. (2001) Covalent alteration of the CYP3A4 active site: evidence for multiple substrate binding domains. *Arch. Biochem. Biophys*. **391**:49-55.

Shear NH, Spielberg SP, Cannon M and Miller M (1988) Anticonvulsant hypersensitivity syndrome. In vitro risk assessment. *J Clin Invest* **82**:1826–1832.

Shou M., Grogan J., Mancewicz J. A., Krausz K. W., Gonzalez F. J., Gelboin H. V., Korzekwa K. R. (1994) *Biochemistry*. **33**: 6450-6455.

Ueng YF, Kuwabara T, Chun YJ, Guengerich FP. (1997) Cooperativity in oxidations catalyzed by cytochrome P450 3A4. *Biochemistry*. **36**:370-381.

Wang RW, Newton DJ, Scheri TD, Lu AY. (1997) Human cytochrome P450 3A4-catalyzed testosterone 6 beta-hydroxylation and erythromycin N-demethylation. Competition during catalysis. *Drug Metab Dispos.* **25**:502-507.

Wang H, Dick R, Yin H, Licad-Coles E, Kroetz DL, Szklarz G, Harlow G, Halpert JR, Correia MA. (1998) Structure-function relationships of human liver cytochromes P450 3A: aflatoxin B1 metabolism as a probe. *Biochemistry*. **37**:12536-45.

Williams PA, Cosme J, Vinkovic DM, Ward A, Angove HC, Day PJ, Vonrhein C, Tickle IJ, Jhoti H. (2004) Crystal Structures of Human Cytochrome P450 3A4 Bound to Metyrapone and Progesterone. *Science*. **305**:683-686.

Wolkenstein P, Tan C, Lecoeur S, Wechsler J, Garcia-Martin N, Charue D, Bagot M, Beaune P. (1998) Covalent binding of carbamazepine reactive metabolites to P450 isoforms present in the skin. *Chem Biol Interact*. **113**:39-50.

Xue L, Wang HF, Wang Q, Szklarz GD, Domanski TL, Halpert JR, Correia MA. (2001) Influence of P450 3A4 SRS-2 residues on cooperativity and/or regioselectivity of aflatoxin B(1) oxidation. *Chem Res Toxicol*. **14**(5):483-91.

Yano JK, Weter MR, Schoch GA. Griffin Kj, Stout CD, Johnson EF. (2004) The structure of human microsomal cytochrome P450 3A4 determined by X-ray crystallography to 2.05-A resolution. *J Biol Chem*. **279**:38091-38094.

Zangar RC, Davydov DR, Verma S. (2004) Mechanisms that regulate production of reactive oxygen species by cytochrome P450. *Toxicol Appl Pharmacol*. **199**:316-31.

FOOTNOTES

‡Present address: Pfizer Global Research & Development, San Diego, CA.

Financial support: This work was supported by NIH grant GM58883 to J.S.L. and M.A.C., NIH grants DK26506 and GM44037 to M.A.C., and NIH grant P30DK26743.

Legends for figures:

Fig. 1. Time-dependent inactivation of CYP3A4-dependent testosterone 6β-hydroxylase activity and concentration-dependent protection by CBZ. CYP3A4 Supersomes™ or functionally reconstituted purified recombinant CYP3A4 was incubated with various concentrations of CBZ (0-1000 μM) and NADPH at 37°C. Aliquots of the mixture were taken at various time intervals (0-30 min) and added to a secondary reaction mixture for the determination of the residual testosterone 6β-hydroxylase activity. **A**. CYP3A4 Supersomes™, CBZ concentration: ♦ 150 μM, ■ 1000 μM; **B**. Functionally reconstituted purified recombinant CYP3A4$(His)_6$, CBZ concentration: ▲ 0 μM, ♦ 10 μM, ● 100 μM, ■ 1000 μM.

Fig. 2. Kinetic profiles of testosterone 6β-hydroxylase activity of CYP3A4 Supersomes™ before or after CBZ-modification. A: Kinetic profile with enzyme preincubation in the absence of both CBZ and NADPH. B: Kinetic profile with enzyme preincubation with CBZ in the absence of NADPH. C: Kinetic profile with enzyme preincubation with CBZ and NADPH. Data shown are the average mean ± SD of three independent experiments.

Fig. 3. Kinetic profiles of testosterone 6β-hydroxylase activity of purified functionally reconstituted CYP3A4$(His)_6$ before or after CBZ-modification. A: Kinetic profile with enzyme preincubation in the absence of both CBZ and NADPH; B: Kinetic profile with enzyme preincubation with CBZ in the absence of NADPH; C: Kinetic profile with enzyme preincubation with CBZ and NADPH. Data shown are the average mean ± SD of three independent experiments.

Fig. 4. Kinetic profiles of erythromycin N-demethylase activity of CYP3A4 Supersomes™ before or after CBZ-modification. A: Kinetic profile with enzyme preincubation in the absence of both CBZ and NADPH. B: Kinetic profile with enzyme preincubation with CBZ in the absence of NADPH. C: Kinetic profile with enzyme preincubation with CBZ and NADPH. Data shown are the average mean ± SD of three independent experiments.

Fig. 5. Docking of carbamazepine (CBZ), testosterone (TS), and erythromycin into the active site of CYP3A4 [Protein Data Bank accession codes 1w0g (Williams et al., 2004)]. Only the helix F-G, helix I, and B-C loop regions are displayed for clarity. Helices are depicted in cyan and loops in tan. **A.** TS molecules are shown in yellow and dark blue stick representations. CBZ molecules bound for carbon 2-adduct is shown in green stick and bound for carbon 3-adduct in orange stick. The side-chain of Cys239 is shown in purple. The heme group is shown in magenta. The linearity of the CYP3A4-dependent CBZ 10,11-epoxidation with time, and our recent findings of the superiority of radiolabeled 3-OHCBZ versus CBZ in CYP3A4 covalent binding after bioactivation lead us to exclude CBZ 10,11-epoxide as the primary reactive intermediate (Pearce et al., 2007). **B.** Same as in A, except that erythromycin, docked in a pose compatible with its N-demethylation, is also shown in a red stick representation. Please note that although these particular dockings are consistent with our *in vitro* kinetic data, they represent an *in silico* attempt at capturing a very dynamic system. Other potential low energy binding modes for the 2nd TS molecule in the CYP3A4 active site outside of the access channel are also possible.

DMD Fast Forward. Published on December 20, 2007 as DOI: 10.1124/dmd.107.016501
This article has not been copyedited and formatted. The final version may differ from this version.

Table 1. Kinetic parameters of (A) Testosterone 6β-hydroxylation by CYP3A4 Supersomes™ and functionally reconstituted purified recombinant CYP3A4 and (B) Erythromycin N-demethylation by CYP3A4 Supersomes™ before and after CBZ-modification.

A.

CYP3A4 Supersomes™	V_{max} (nmol/min/nmol)	K_m (μM)	Hill coefficeint (n)
NADPH-, CBZ-	46.5 ± 1.6	40.6 ± 4.2	1.2 ± 0.1
NADPH-, CBZ+	33.3 ± 1.5	36.7 ± 5.3	1.3 ± 0.2
NADPH+, CBZ+	37.1 ± 1.9	59.3 ± 9.7	1.0 ± 0.1
Purified CYP3A4			
NADPH-, CBZ-	12.2 ± 0.3	81.5 ± 4.3	1.4 ± 0.1
NADPH-, CBZ+	11.2 ± 0.4	102.3 ± 8.6	1.2 ± 0.1
NADPH+, CBZ+	7.2 ± 0.6	132.4 ± 26.1	1.1 ± 0.1

B.

CYP3A4 Supersomes™	Vmax (nmol/min/nmol)	Km (μM)
NADPH-, CBZ-	3.27 ± 0.08	44.0 ± 4.0
NADPH-, CBZ+	3.60 ± 0.58	80.0 ± 0.00
NADPH+, CBZ+	3.61 ± 0.22	44.0 ± 4.0

NADPH-, CBZ-: Preincubation of CYP3A4 in the absence of NADPH and CBZ followed by assay of either testosterone 6β-hydroxylase activity (A) or erythromycin N-demethylase (B); NADPH-, CBZ+: Preincubation of CYP3A4 with CBZ but without NADPH followed by assay of either testosterone 6β-hydroxylase activity (A) or erythromycin N-demethylase (B); NADPH+, CBZ+: Preincubation of CYP3A4 in the presence of both NADPH and CBZ followed by assay of either testosterone 6β-hydroxylase activity (A) or erythromycin N-demethylase (B).

DMD Fast Forward. Published on December 20, 2007 as DOI: 10.1124/dmd.107.016501
This article has not been copyedited and formatted. The final version may differ from this version.

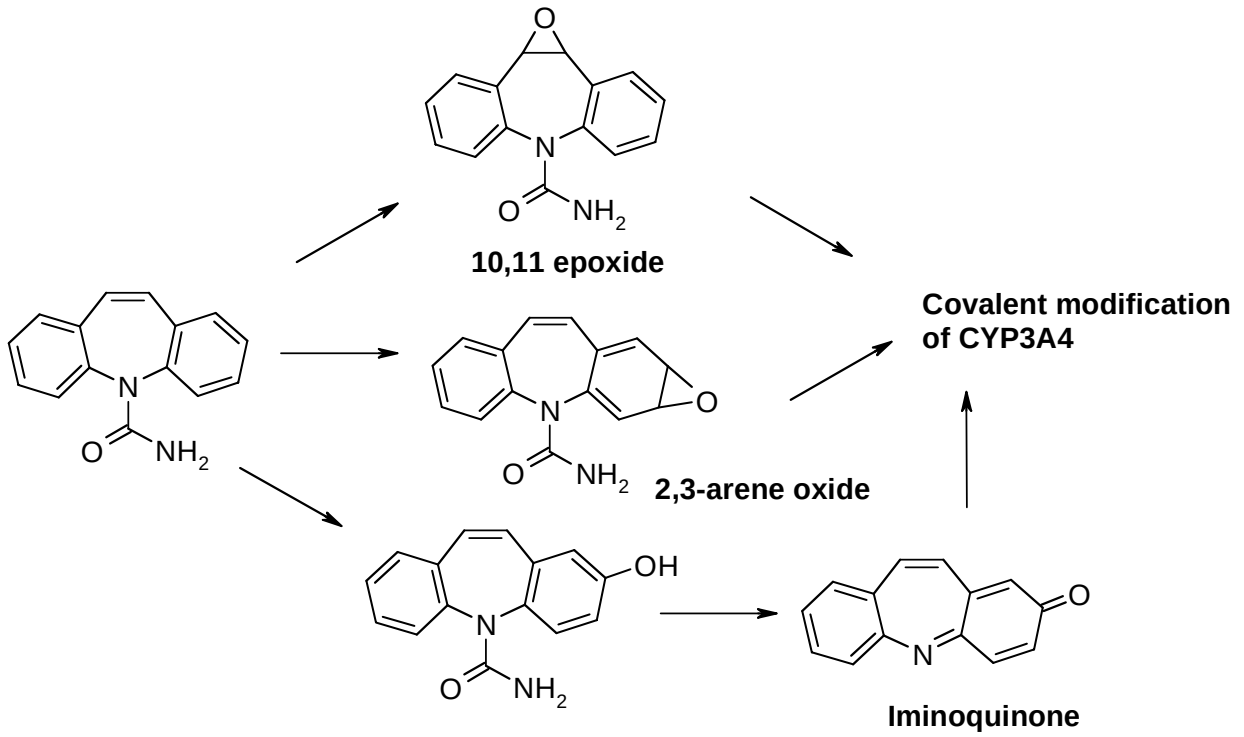

Scheme 1. Proposed reactive metabolites and the covalent modification of CYP3A4 active site. The iminoquinne is reportedly derived from 2-hydroxycarbamazepine (Pearce et al, 2005). Other reactive metabolites include 2,3 arene oxide, 2,3 catechol, dihydroquinone and the 3-quinone methide.

Figure 1

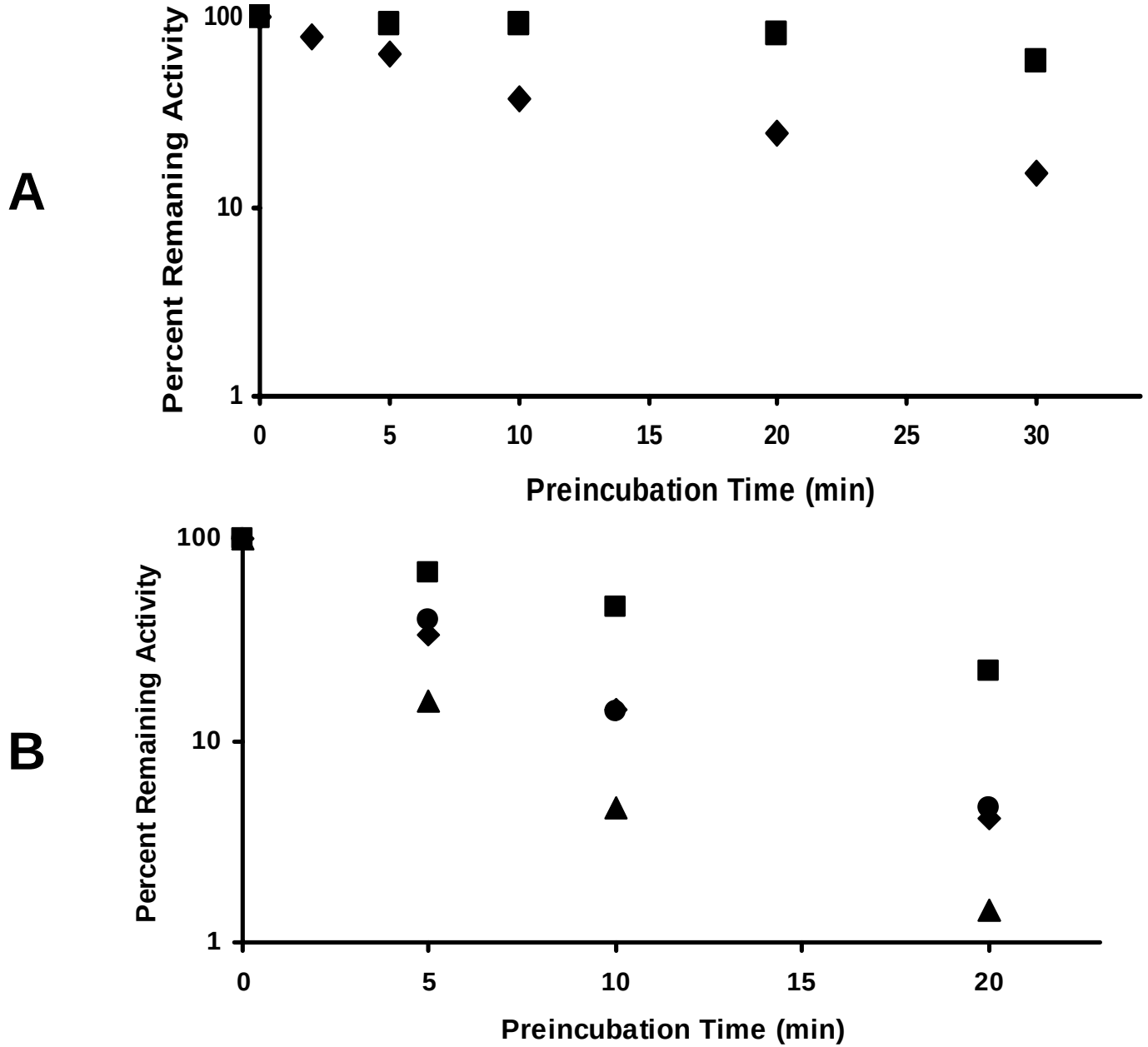

Fig. 2A

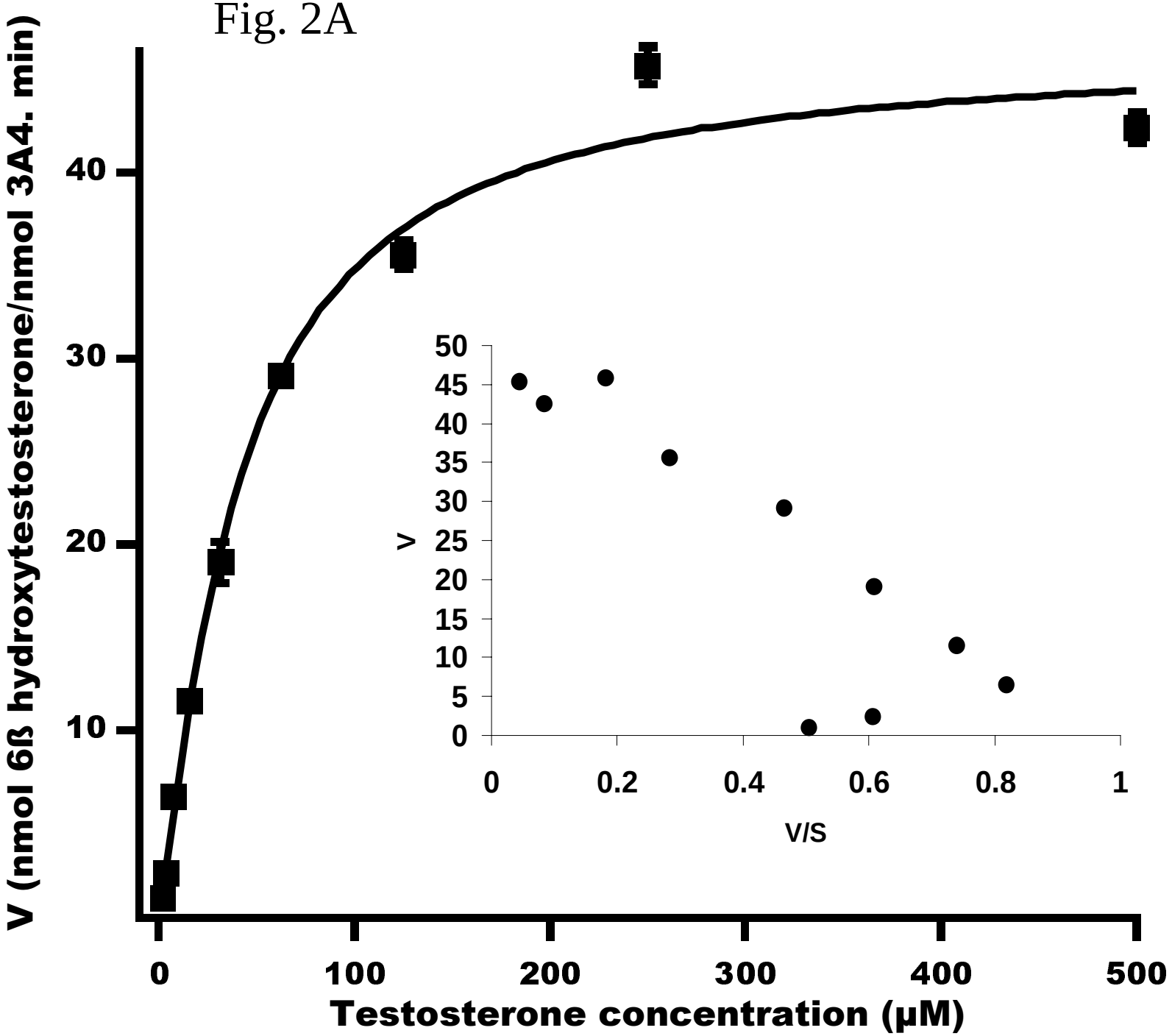

Fig. 2B

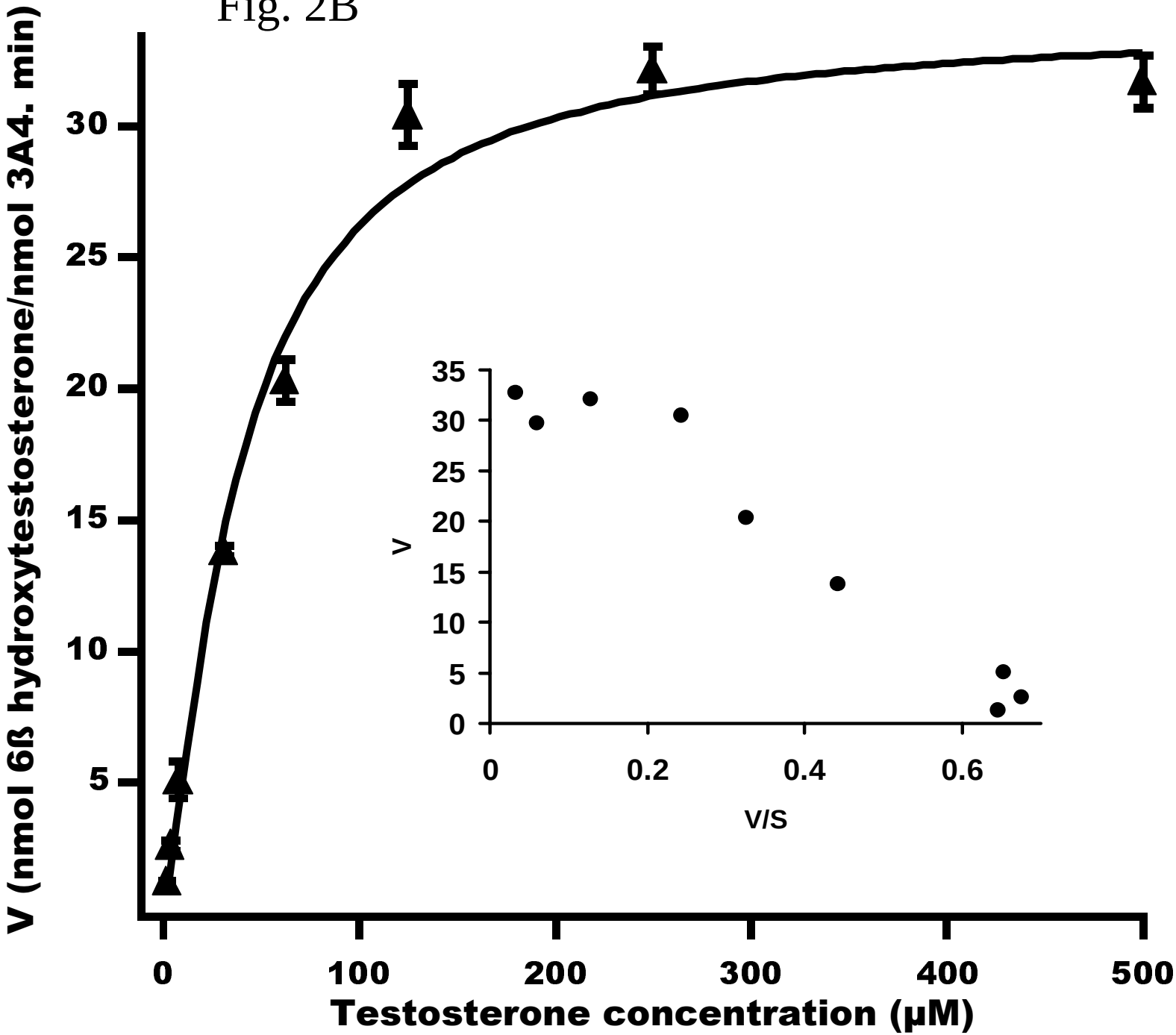

Fig. 2C

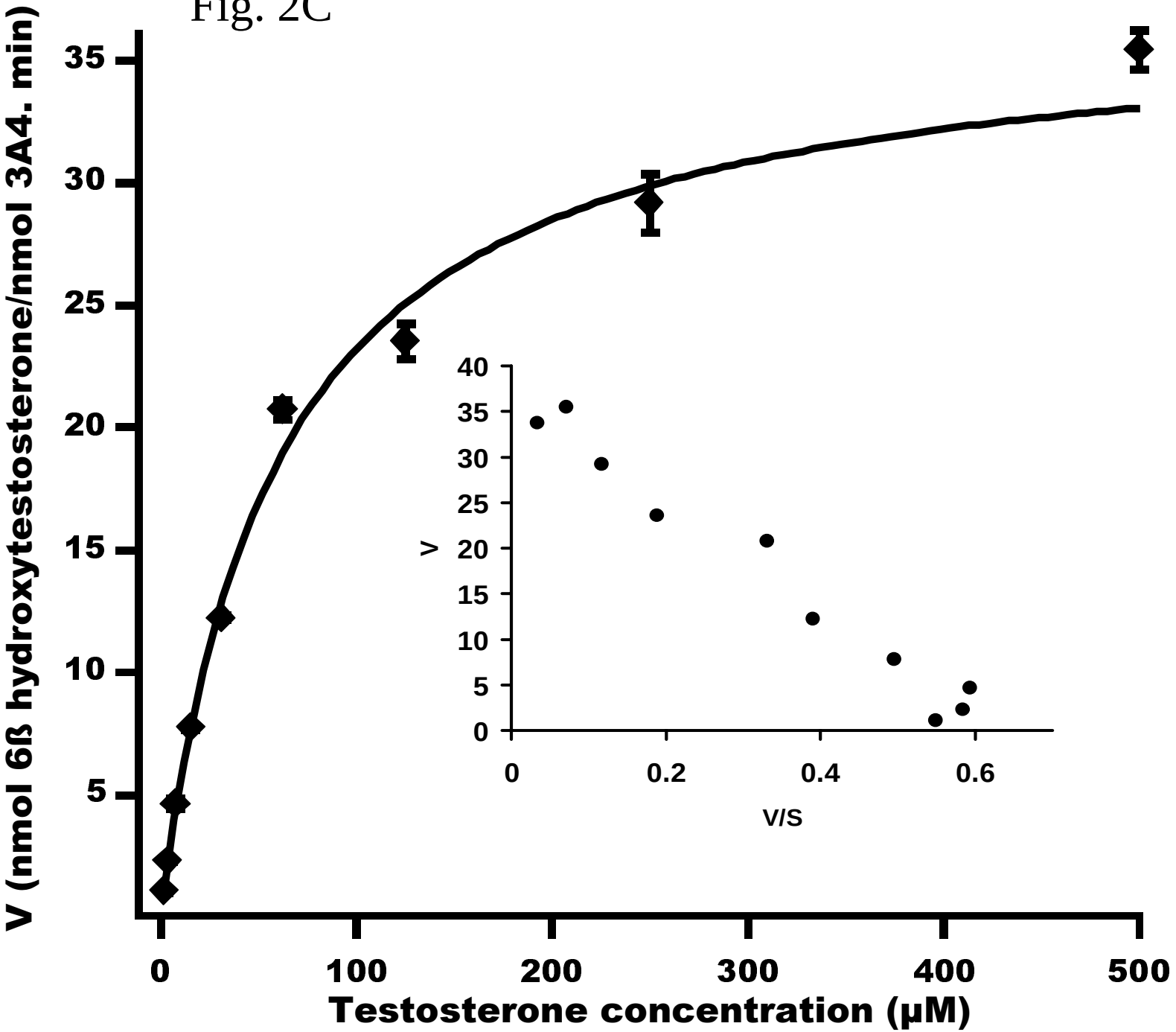

Fig. 3A

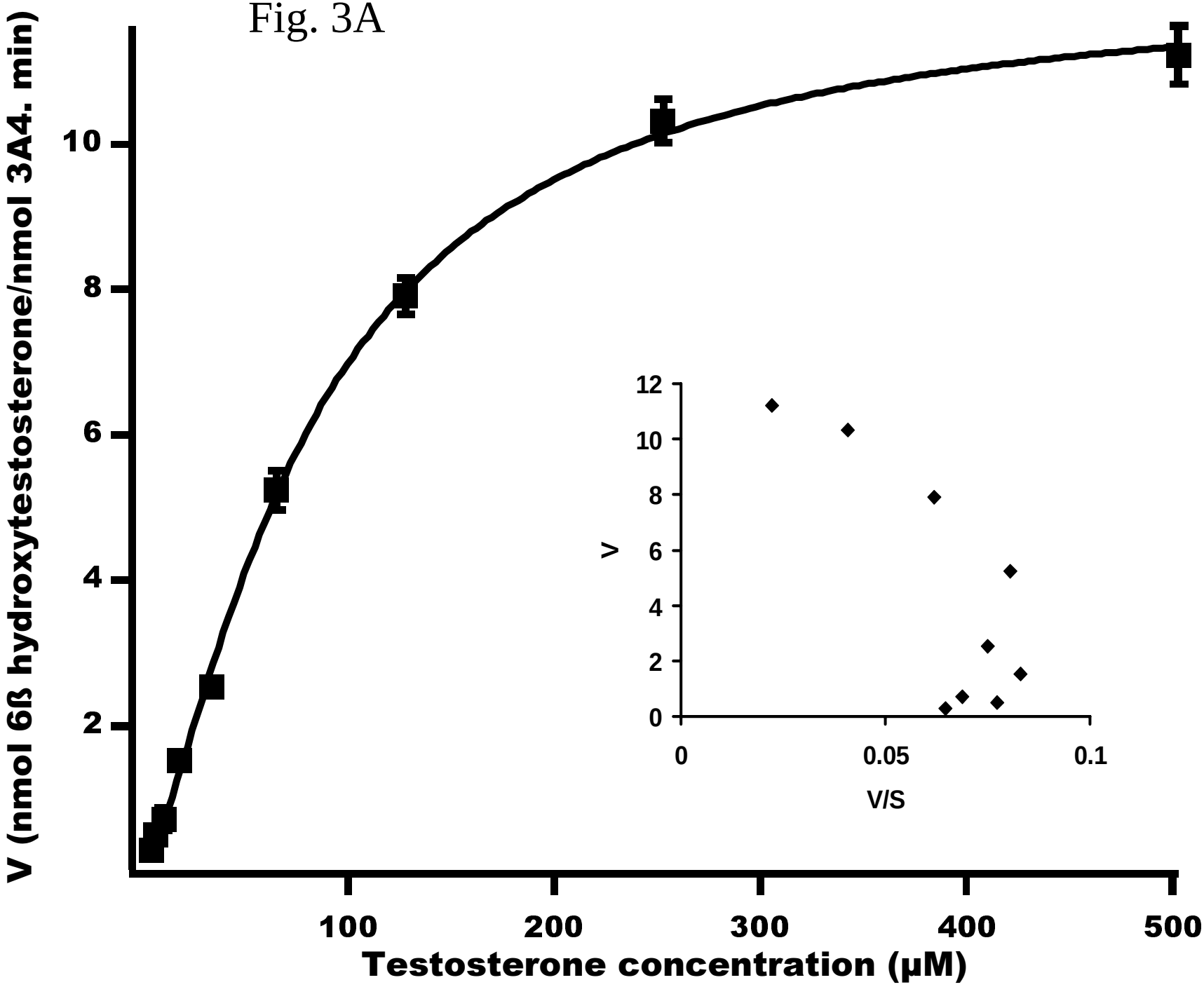

Fig. 3B

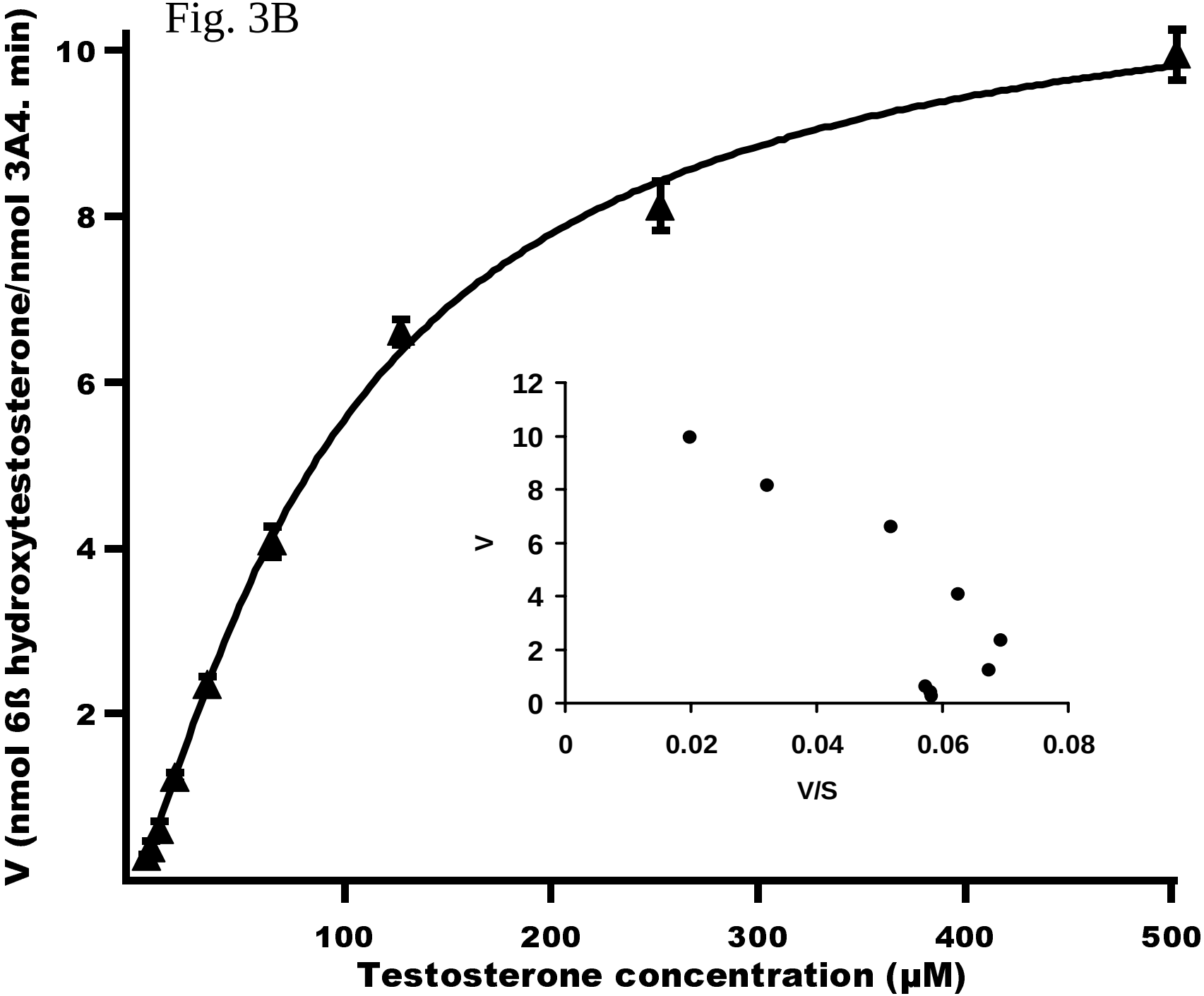

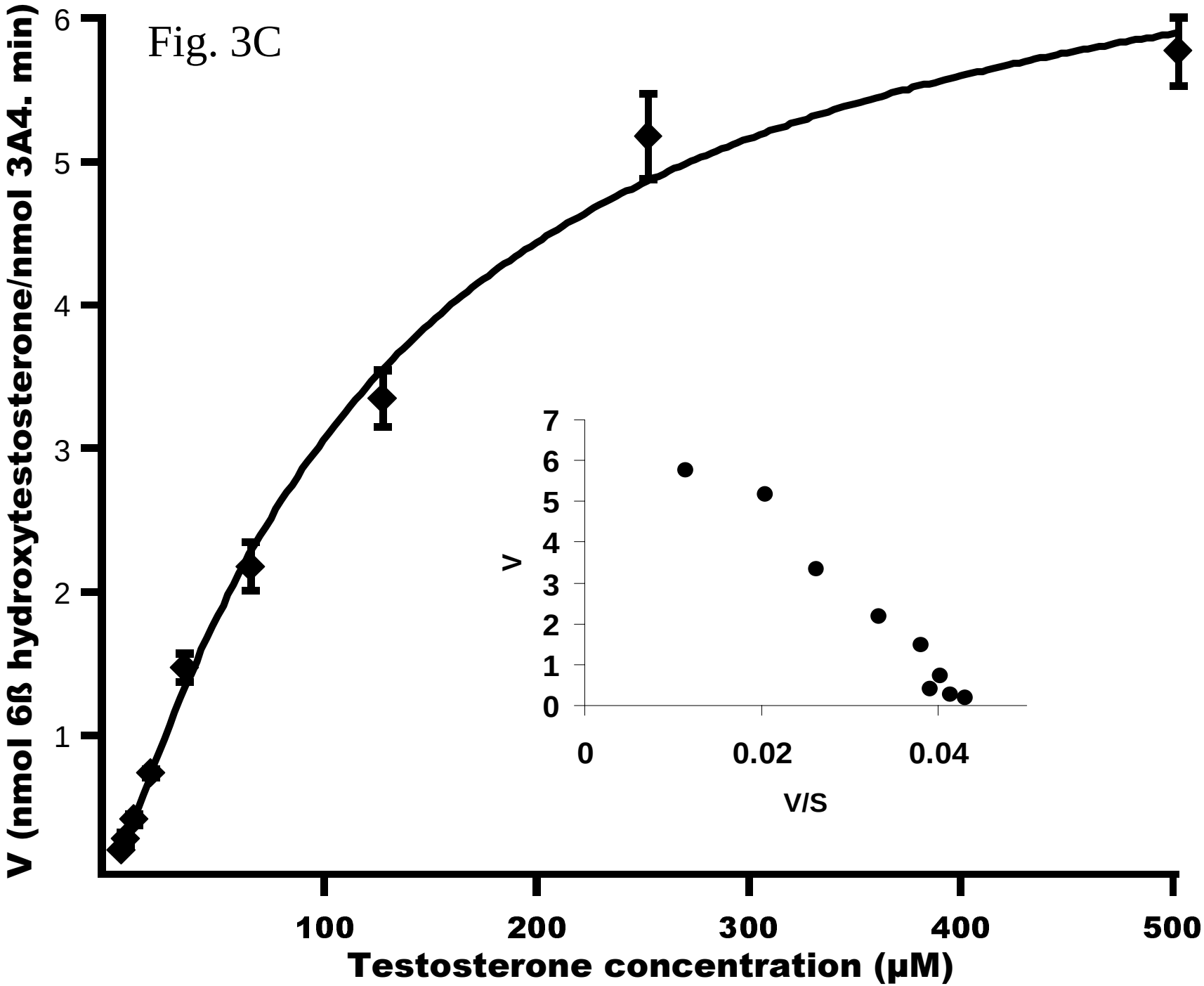

Fig.4A

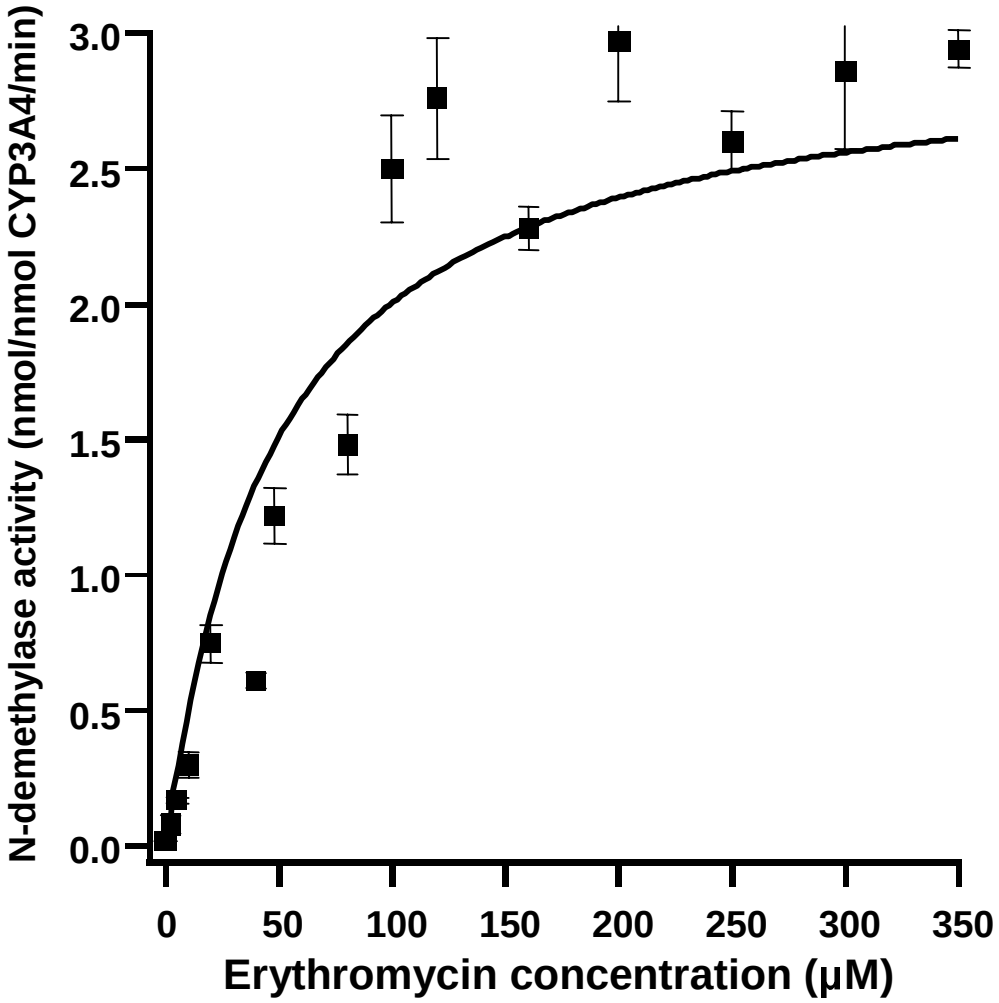

Fig.4B

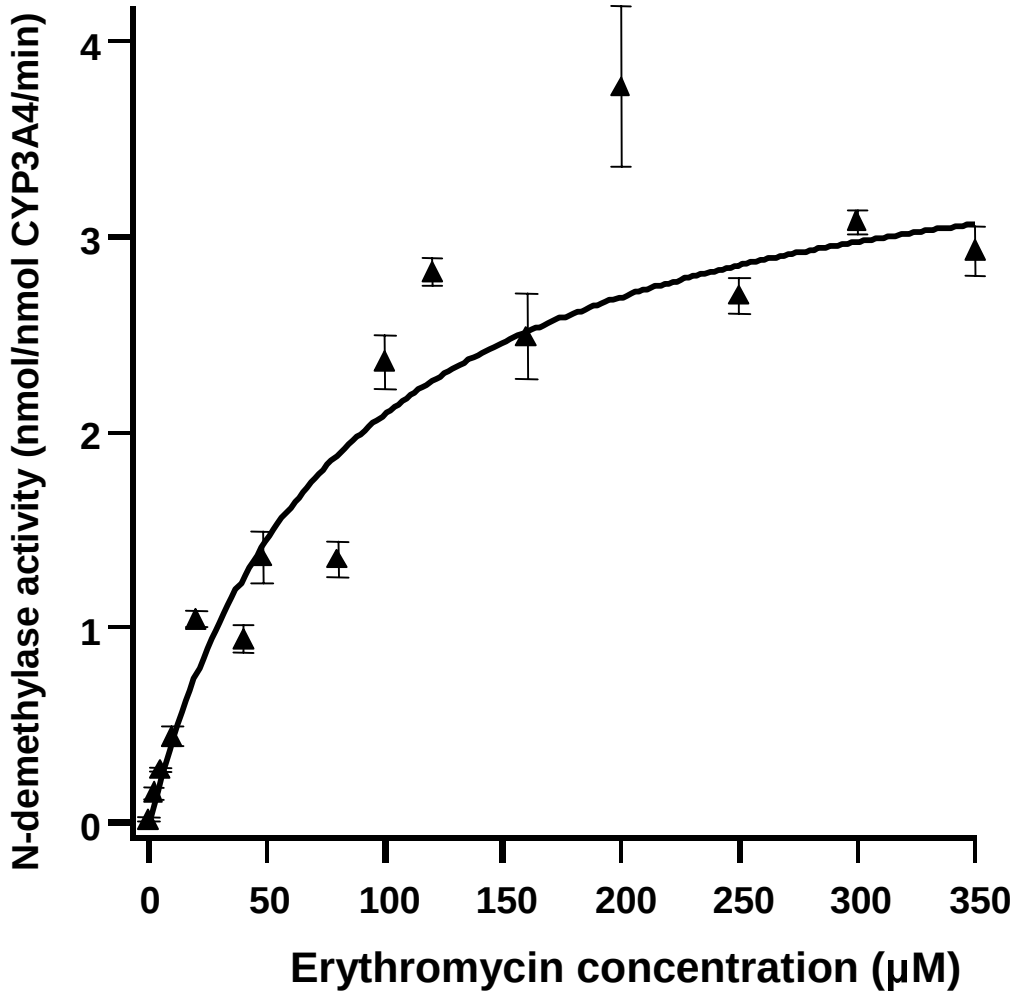

Fig.4C

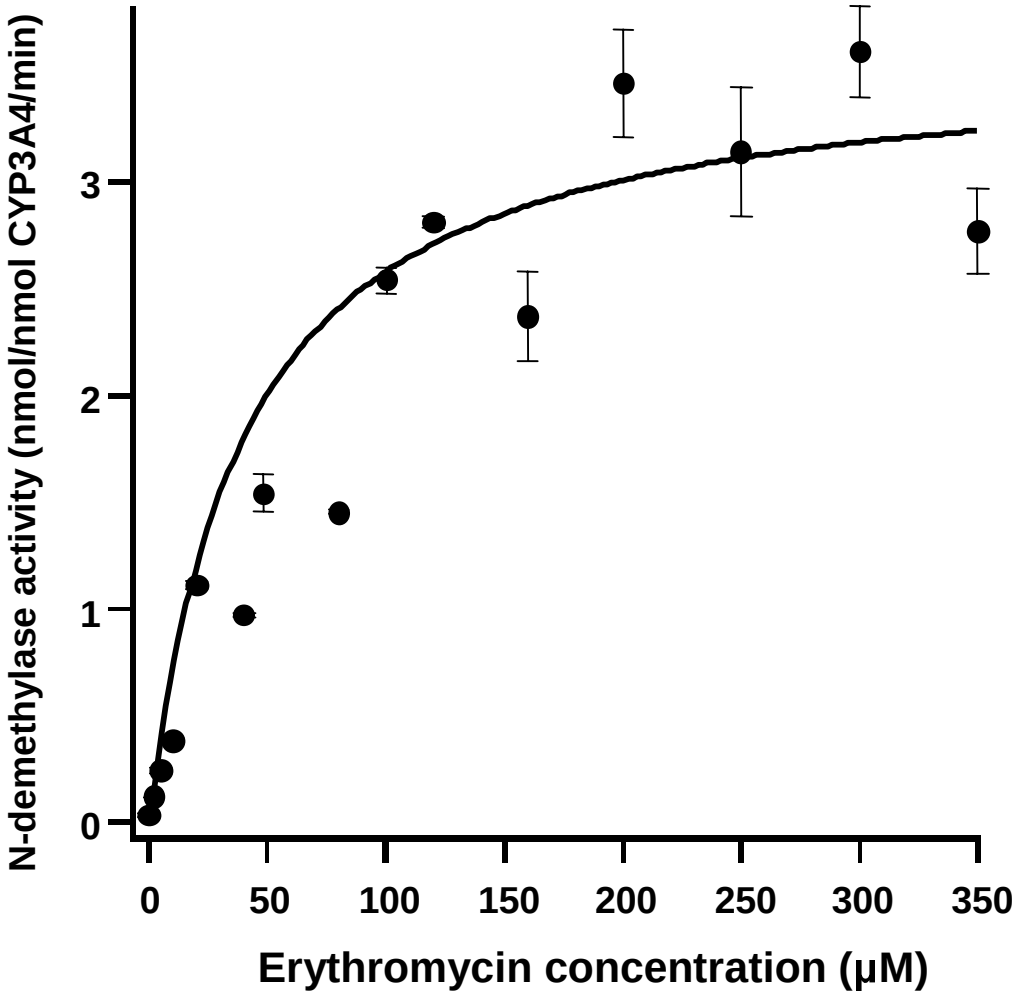

Fig.5A

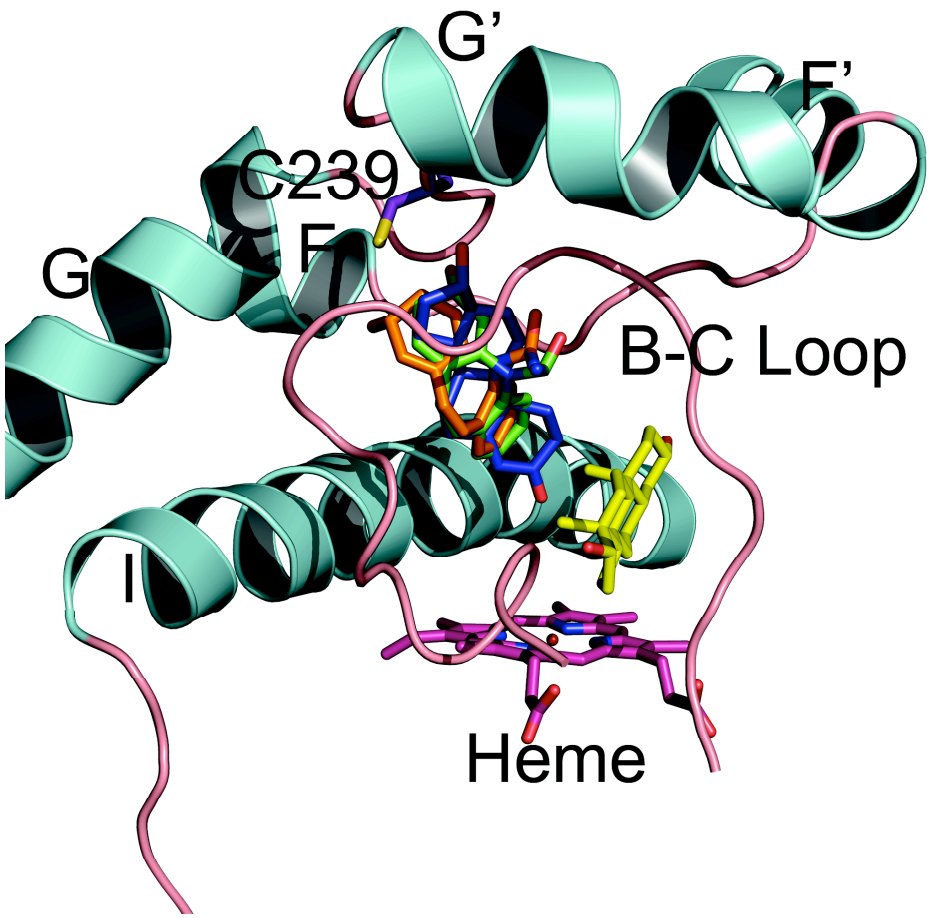

Fig. 5B